Research Square

Preprints are preliminary reports that have not undergone peer review.
They should not be considered conclusive, used to inform clinical practice,
or referenced by the media as validated information.

Hippocampal Glial Signatures of Cognitive Resilience in SuperAgers with Primary Age- Related Tauopathy

Caroline Nelson
Northwestern University
Rachel Keszycki
Northwestern University
Ivan Ayala
Northwestern University
Antonia Zouridakis
Northwestern University
Grace Minogue
Northwestern University
Allegra Kawles
Northwestern University
Alyssa Macomber
Northwestern University
Erfan Taefi
Northwestern University
Pouya Jamshidi
Northwestern University
Sandra Weintraub
Northwestern University
Rogan A. Grant
Northwestern University
Sarah Doran
Northwestern University
Jamie Walker
Icahn School of Medicine at Mount Sinai
Rudy J. Castellani
Northwestern University
Molly A. Mather
Northwestern University
M-Marsel Mesulam

Northwestern University

Changiz Geula

Northwestern University

Tamar Gefen

tamar.gefen@northwestern.edu

Northwestern University

Article

Keywords: primary age-related tauopathy, glial reactivity, cognitive aging, hippocampus, SuperAger

Posted Date: November 16th, 2026

DOI: https://doi.org/10.21203/rs.3.rs-11578733/v1

License: This work is licensed under a Creative Commons Attribution 4.0 International License.
Read Full License

Additional Declarations: No competing interests reported.

ORIGINAL RESEARCH

Hippocampal Glial Signatures of Cognitive Resilience in SuperAgers with Primary Age-Related Tauopathy

Caroline Nelson[1], Rachel Keszycki[1,2], Ivan Ayala[1], Antonia Zouridakis[1,2], Grace Minogue[1,2], Allegra Kawles[1,2], Alyssa Macomber[1,2], Erfan Taefi[1], Pouya Jamshidi[1], Sandra Weintraub[1,2], Rogan A. Grant[3], Sarah Doran[1], Jamie Walker[4], Rudy J. Castellani[1], Molly A. Mather[1,2], M-Marsel Mesulam[1], Changiz Geula[1], and Tamar Gefen[1,2]

[1]Mesulam Institute for Cognitive Neurology and Alzheimer's Disease, Feinberg School of Medicine, Northwestern University, Chicago, IL
[2]Department of Psychiatry and Behavioral Sciences, Northwestern Feinberg School of Medicine, Chicago, Illinois, USA
[3]Division of Pulmonary and Critical Care Medicine, Department of Medicine, Feinberg School of Medicine, Northwestern University, Chicago, IL
[4]Department of Pathology, Molecular and Cell-Based Medicine, Icahn School of Medicine at Mount Sinai, New York, NY, USA

Key Words: primary age-related tauopathy; glial reactivity; cognitive aging; hippocampus; SuperAger

Send correspondence to:
Tamar Gefen, PhD
Mesulam Institute for Cognitive Neurology and Alzheimer's Disease
Northwestern University Feinberg School of Medicine
300 E. Superior Street, Tarry Building, 8th Floor, Chicago, IL 60611

E-mail: tamar.gefen@northwestern.edu
Phone: (312) 695-9627

Funding: This study was supported by grants from the National Institute on Aging (P30 AG013854, P30 AG072977, R01 AG062566, R01 AG077444, R01 AG056258, R56 AG075600, T32 AG020506), National Institute of Neurological Disorders and Stroke (R01 DC008552), the Gefen-Querrey Brain Health Endowment, the National Science Foundation's Graduate Research Fellowship (DGE-1842165), the Karen Toffler Charitable Trust, the Schmidt Science Fellowship, in partnership with Rhodes Trust, and the Simpson Querrey Fellowship in Data Science.

Conflicts of Interest: The authors have no duality or conflicts of interest to declare.

Acknowledgements: We are grateful to our research participants for their invaluable contributions to scientific discovery.

ABSTRACT

Cognitive SuperAgers are individuals age 80+ with episodic memory equal to or better than individuals 20-30 years their junior. Prior investigations of SuperAgers reveal significantly lower microglial activation in neocortical white matter and reduced neurofibrillary tangle burden compared to their age-matched, cognitively-average peers. Primary age-related tauopathy (PART), defined by neurofibrillary tangles confined to the medial temporal lobe and sparse or absent amyloid-β plaques, is relatively common in cognitively normal controls. In a cohort of SuperAgers and cognitively normal controls with PART, we examined glial immunoreactivity in grey and white matter hippocampal subregions. Nineteen participants (N=9 SuperAgers; N=10 age-matched cognitively-average controls) with postmortem PART were identified from the Northwestern ADRC brain bank. Paraffin-embedded hippocampal sections were immunohistochemically stained with AT-8 (pTau), GFAP (astrocytic reactivity), HLA-DR (microglial activation), and Olig2 (oligodendrocytes). Percent area of immunoreactivity was quantified across hippocampal grey and white matter subregions (CA1-3 and dentate gyrus) and layers (molecular layers of the dentate gyrus, radiatum, oriens, alveus, and fimbria). SuperAgers and controls with PART showed similar hippocampal pTau burden. Relative to their peers with average memory capacity, SuperAgers displayed heightened overall astrocytic GFAP reactivity in grey and white matter ($p<0.05$), lower microglial activation in white matter ($p<0.05$), and increased Olig2 density particularly in the fimbria ($p<0.01$). Across the entire cohort, there was an inverse relationship between pTau and astrocytic immunoreactivity. There are two major findings in this study. First, that PART is compatible with youthful memory capacity in advanced old age. Second, that there is a glial signature associated with this feature. We speculate that the glial environment may have prevented or mitigated the gradual loss of memory capacity that would be expected in advanced age with PART pathology.

INTRODUCTION

Age is the most significant risk factor for developing Alzheimer's disease neuropathologic change (ADNC), typically characterized by neurofibrillary tangles (NFTs) and amyloid-β (Aβ) plaques. However, NFTs may also present without significant Aβ pathology. First described in 1992 [51], this phenomenon has since been extensively characterized [3, 28, 27, 40] and formally termed "primary age-related tauopathy" (PART; Crary et al., 2014). PART is defined by NFTs confined to the medial temporal lobe in Braak stage IV (limbic) or lower [9] and minimum or absent Aβ plaques [15]. Individuals with PART tend to be older at time of death than individuals with ADNC, FTLD-TDP, ALS, or FTLD-tau [26]. Individuals with a primary neuropathologic diagnosis of PART also typically tend to be cognitively unimpaired [25, 26, 40]. Mechanistically, studies indicate a selective vulnerability of CA2 hippocampal subregion to early PART pathology, a subregion typically resistant to ADNC pathology until later disease stages [6, 52]

Our group has previously found various biological signatures that define SuperAgers, identified as individuals age 80+ with episodic memory equal to or better than individuals 20-30 years their junior [53]. The hippocampus, in particular, is one of the primary sites of distinctive SuperAging features: compared to same-age peers, the region displays lower NFT burden [41, 20]; larger stellate neurons of the entorhinal cortex, the primary source of input to the hippocampus [35]; and elevated neurogenesis in the granule cell layer of the dentate gyrus supported by an enriched astrocytic environment [16]. One study showed that in cortical white matter, SuperAgers exhibited reduced microglial activation compared to age-matched cognitively average-for-age controls, at levels that were comparable to individuals 20-30 years their junior [21]. Based on findings of glial differences, the current study examined glial immunoreactivity in grey and white matter hippocampal subregions in a unique group of brain specimens from SuperAgers and age-matched, cognitively normal-for-age controls, all with PART. By characterizing patterns of astrocytic, microglial, and oligodendrocytic immunoreactivity in the hippocampus, we identified a unique pattern of glial distribution in SuperAgers with PART pathology that may represent a potential substrate of their superior memory performance despite aggregation of tau pathology in this region.

MATERIALS AND METHODS

Participant Characteristics.

Written informed consent was obtained from all participants, and the study was approved by the Northwestern University Institutional Review Board and in accordance with the Helsinki Declaration. SuperAgers are defined as individuals age 80 or older with episodic memory performance equal to or better than normative performance of individuals in their 50s to 60s [42]. The delayed recall score of the Rey Auditory Verbal Learning Test (RAVLT) [47] was used as a measure of episodic memory. SuperAgers were required to obtain a delayed recall score of ≥9 words on the RAVLT [54, 23]. A 30-item version of the Boston Naming Test (BNT-30; [46]), Trail-Making Test Part B (TMT Part B; [39]), and Category Fluency test ("Animals;" [34] were used to measure cognitive function in nonmemory domains. On the BNT-30, TMT Part B, and Category Fluency, SuperAgers were required to perform within or above 1 standard deviation (SD) of the average range for their age and education according to published psychometric norms [29, 24, 48]. By contrast, normal controls were age 80 or older and were required to fall within 1 SD of the average range for their age and education according to published psychometric norms on the same memory and nonmemory neuropsychological measures [29, 24, 48]. These criteria are in accordance with the National Institute on Aging and Alzheimer's Association (NIA-AA) guidelines for elderly individuals considered "not demented" [1]. Refer to [53] for more details. Nineteen autopsied participants with a primary pathologic diagnosis of PART (SuperAgers, N=9; normal controls, N=10) were identified from the Northwestern University Alzheimer's Disease Research Center Brain Bank. All participants were community-dwelling, English-speaking adults ≥80 years of age without significant neurologic or psychiatric illness from study enrollment to death as determined through annual neuropsychological assessment.

Neuropathological Evaluation.
All participants indicated intent for brain donation at annual study visits; consent for brain-only autopsy was obtained from legally authorized next-of-kin at the time of death. All brains underwent extensive postmortem neuropathological evaluation and received a primary pathological diagnosis of PART by a board-certified neuropathologist (RC and PJ) in accordance with published criteria [15, 25]. At autopsy, brains were divided along the midsagittal plane, cut into 2–3 cm coronal blocks, fixed in 4% paraformaldehyde for 36 hours or formalin for 2 weeks, taken through sucrose gradients (10–40% in 0.1 m sodium phosphate buffer with 0.02% sodium azide, pH 7.4) for cryoprotection, and stored at 4°C. In accordance with PART diagnostic criteria [15, 25], amyloid β (Aβ) burden was limited to Thal phase 2 (allocortex) or lower [49], and neurofibrillary tangle (NFT) involvement was limited to Braak stage IV (limbic) or lower [9]. Cases with extensive neocortical tau pathology indicative of other primary tauopathies (e.g., frontotemporal lobar degeneration with tau) were excluded. One SuperAger (SA9) had comorbid argyrophilic grain disease (AGD) [56]. No participants had comorbid aging-related tau astrogliopathy (ARTAG) [30]. Apolipoprotein E (ApoE) genotype was available for 14 participants. No participants had a known mutation associated with AD or FTLD (e.g., MAPT). See **Table 1** for participant characteristics.

Table 1 Characteristics of SuperAging and Normal Control Participants with PART as Primary Neuropathologic Diagnosis.

Participant	*Age at death (years)*	*Sex*	*PMI (h)*	*Brain weight (g)*	*Braak Stage*	*Thal Phase*	*ApoE*	*Comorbid pathology*
SA1	90	F	4.5	1100	III	0	2,3	Vascular disease with motor microinfarcts
SA2	90	M	9	1120	I	0	3,3	Mild to moderate vascular disease
SA3	84	F	90	1289	II	0	3,3	Remote ischemic infarct, Wallerian degeneration
SA4	90	F	9	1133	III	1	3,3	Mild vascular disease
SA5	90	M	14	1267	II	1	3,4	Moderate vascular disease
SA6	87	M	67	1243	II	2	3,3	
SA7	98	F	4	1175	III	2	3,3	Hypertensive cerebrovascular disease
SA8	85	F	9	1310	III	0	3,3	Moderate vascular disease
SA9	97	F	48.0	1127	III	0	3,3	AGD; Moderate vascular disease
NC 1	90	F	NA	1290	II	0	2,3	Acute infarcts
NC 2	83	F	NA	NA	I	0	NA	
NC 3	95	M	45	1421	III	1	3,3	
NC4	95	M	36	1270	II	1	3,3	Moderate vascular disease

NC 5	93	F	9	1180	III	2	3,3	Vascular disease
NC 6	89	F	9	NA	II	1	NA	
NC 7	98	M	12	NA	II	1	NA	
NC 8	87	F	10	1300	III	1	NA	History of seizures
NC 9	107	F	8	NA	II	1	NA	
NC 10	92	F	12	1314	IV	0	2,4	

SA, SuperAger; NC, normal control; PART, primary age-related tauopathy; PMI, post-mostem interval; AGD, argyrophilic grain disease; NA, not available; F, female; M, male; h, hours; g, grams; ApoE, Apolipoprotein E. Braak staging followed published guidelines [7, 8, 10]. Thal phase followed published guidelines [49]

Tissue Processing and Histopathology.
Blocks of hippocampal tissue were embedded in paraffin and serially sectioned at 5 µm thickness for immunohistochemical staining. AT-8 antibody for human tau phosphorylated at Ser202/205 (mouse monoclonal; Invitrogen MN1020; RRID: AB_223647; 1/500) was used to visualize phosphorylated tau (pTau) accumulation. Glial fibrillary acidic protein (GFAP) was used to quantify reactive astrocytes (rabbit monoclonal; Abcam ab68428; RRID: AB_1209224; 1/800). HLA-DR antibody was used to visualize proinflammatory microglia and other immune cells (rabbit monoclonal; Invitrogen MA5-32232; RRID: AB_2809518; 1/100). An antibody against oligodendrocyte transcription factor 2 (Olig2) was used to quantify oligodendrocytes and oligodendrocyte precursor cells (OPCs; rabbit monoclonal; Abcam ab109186; RRID:AB_10861310; 1/100). Slides were developed manually using 3,3'-Diaminobenzidine (DAB) as chromogen. **Fig. 1** depicts immunohistochemical stains. A 1.0% cresyl violet Nissl stain was used to visualize neuron morphology for manual annotation of hippocampal subregions and their respective laminar boundaries (**Fig. 2**).

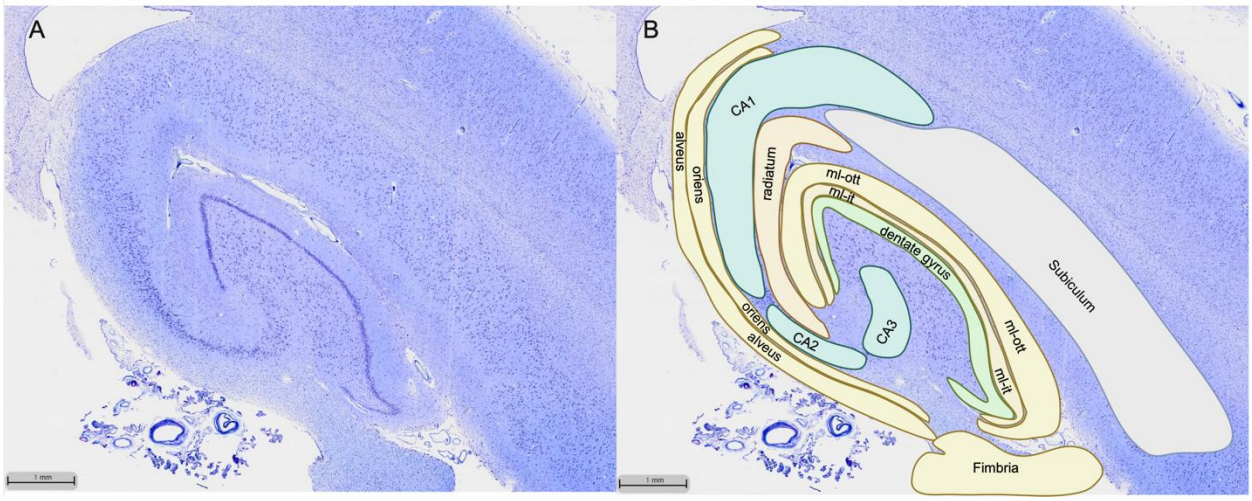


Fig. 2 Hippocampal Subregions of Interest. A) Photomicrograph of a SuperAger's hippocampus stained with CV to visualize neurons. **B)** Annotations of the hippocampal subregions of interest are demonstrated [43, 55]. Grey matter subregions (green) include the CA1, CA2, and CA3, consisting of pyramidal cells (teal), and the granule cells of the dentate gyrus (light green). White matter layers are depicted in yellow. Directly above the granule layer is the inner third of the molecular layer of the dentate gyrus (ml-it), surrounded by the stratum lacunosum-moleculare layer (ml-ott). The stratum radiatum (radiatum) abuts the

CA1 and CA2 subregions. The axonal projections of the pyramidal cells are primarily found in the stratum oriens (oriens) and the medial adjacent alveus, which then bundle to form the fimbria. The fimbria is the medial hippocampus white matter bundle that travels posterior-superiorly to form the crus of the fornix. Scale bar = 1 mm

Imaging Acquisition and Analysis.
Hippocampal sections were digitally imaged in brightfield at 20x magnification using an Olympus V200 slide scanner system (Olympus, Tokyo, Japan) and analyzed using HALO image analysis software (v4.0.1, Indica Labs). AI classifier training was performed across all slides per stain. Corresponding output values were used to create a final set of parameters by which every slide was analyzed (**Fig. 1**) to obtain percent area occupied (%AO) by each stain. Values outside ±1 SD of the mean of their pathological group underwent manual quality control for accuracy, in line with prior methods [33]. Collaborators may request digital images and optimized protocols derived from post-mortem histological analysis of participants upon approved request (see: https://www.brain.northwestern.edu/scientists-students/collaborative-request.html). Briefly, for each slide, grey and white matter subregions of interest were annotated manually in HALO based on previously established observations and criteria [43, 55] (**Fig. 2**). Grey matter subregions included the Cornu Ammonis subfields (CA1, CA2, CA3), and granule cell layer of dentate gyrus (DG). White matter layers included the molecular layer of the dentate gyrus, which was subdivided into the inner third (ml-it) and outer two-thirds (ml-ott); stratum radiatum (radiatum); stratum oriens (oriens); alveus; and fimbria. Images of hippocampi were then analyzed for the percent area occupied (%AO) by immunoreactivity of each antibody within each hippocampal subregion of interest using the HALO MiniNet Classifier AI algorithm **(Fig. 1)**.

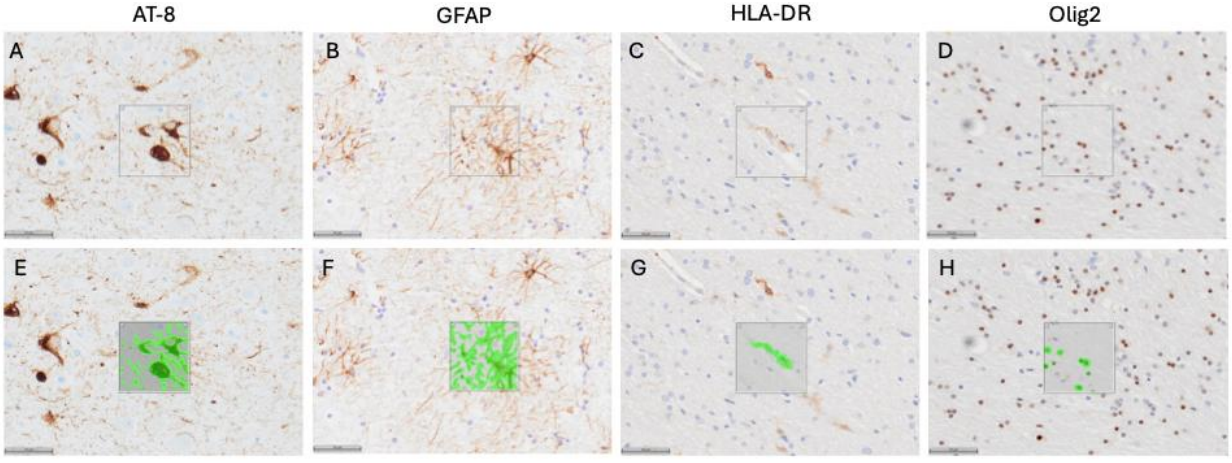


Fig. 1 Immunostaining for phosphorylated tau and glial response in the hippocampus in PART. Photomicrographs of hippocampal staining for AT-8 **(A, E),** GFAP **(B, F),** HLA-DR **(C, G)**, and Olig2 **(D, H)** are depicted in the top row. The bottom row depicts corresponding overlays of the HALO MiniNet Classifier AI algorithm. Scale bar = 50 μm

Statistical Analysis.
To facilitate comparisons across morphologically disparate glial and tau immunoreactivity patterns, statistical analysis was performed on log-transformed data using the formula $\log_{10}$ (%AO + 1). Multilevel mixed-effects models were used to compare subregional %AO per each immunoreactive marker (AT-8, GFAP, HLA-DR, and Olig2) as well as subregional differences between SuperAgers and normal controls. Bonferroni correction was used for multiple comparisons for all post-hoc analyses. Multilevel mixed-effects models were also used to compare subregional %AO across stains, including random intercepts for subject to account for within-case clustering across regions. Generalized estimating equations (GEE) were used to investigate the relationship between %AO of phosphorylated tau (AT-8) and age at death, as well as phosphorylated tau (AT-8) and glial immunoreactivity (GFAP, HLA-DR, and Olig2). GEEs accounted for clustered data and investigated potential covariates such as age at death and presence of Aβ. Complementary post-hoc regression analyses were performed to obtain correlation coefficients (R^2). Fisher's exact tests were used to compare ApoE ε4 allele frequency, Braak stage, sex, presence of Aβ plaques, and Thal phase between SuperAgers and normal controls. T-tests were used to compare age at death, postmortem interval (PMI), brain weight, and education between SuperAgers and the normal control group. Analysis was performed via Stata 19 (Stata Statistical Software 19, StataCorp, College Station, Texas, USA).

RESULTS.

Cohort Demographics.

Sixty-eight percent of participants were female, with similar frequencies between groups (SuperAgers = 66%, normal controls = 70%). Average age at death was 91.58 years (SD = 5.82). Braak staging ranged from I-III in SuperAgers and I-IV in normal controls. Aβ was present in 44% of SuperAgers and 60% of normal controls, and Thal scores ranged from 0-2 in both groups. Two participants, one SuperAger and one control, had a single ApoE ε4 allele, the strongest known genetic risk factor for Alzheimer's disease (AD) [14, 18, 11], and three participants had at least one ApoE ε2 allele, a proposed protective allele against AD [13, 38]. There were no significant differences in average PMI, brain weight, age at death, education level, frequency of APOE ε4 allele, the presence of postmortem Aβ plaques, or Thal phase between SuperAgers and normal controls (see **Table 1**).

Grey Matter Vulnerability to Tau and Glial Cell Density in PART Differs by Hippocampal Subregion.
We observed that pTau accumulation was confined to the grey matter and therefore did not assess this parameter in white matter layers. Across all participants, grey matter pTau (%AO by AT-8), was significantly higher in the CA1 (μ=0.89, SD=0.53) and CA2 (μ=0.89, SD=0.49) versus the CA3 (μ=0.21, SD=0.19) by ~4-fold magnitude and the DG (μ=0.14, SD=0.17) by ~6-fold magnitude (both $p<0.0001$). See **Fig. 3A.** Grey matter HLA-DR+ activated microglia were significantly more abundant in CA2 (μ=0.61; SD=0.48) than in CA1 (μ=0.46; SD=0.44) and CA3 (μ=0.47; SD=0.37) ($p<0.01$), by approximately 30% (**Fig. 3B).** Astrocytic reactivity (%AO by GFAP) was significantly higher in the DG (μ=1.18, SD=0.50) and CA3 (μ=0.98, SD=0.54) grey matter compared to the CA1 (μ=0.54; SD=0.48) and CA2 (μ=0.69; SD=0.49) ($p<0.001$), by ~1.5-2-fold (**Fig. 3C**). Grey matter oligodendrocyte density (%AO by Olig2+) was significantly higher in the CA2 (μ=0.36; SD=0.35) and CA3 (μ=0.36; SD=0.37) than in the DG (μ=0.12; SD=0.11) ($p<0.001$), and CA1 (μ=0.21; SD=0.17) ($p<0.05$) by ~2-3-fold (**Fig. 3D**).

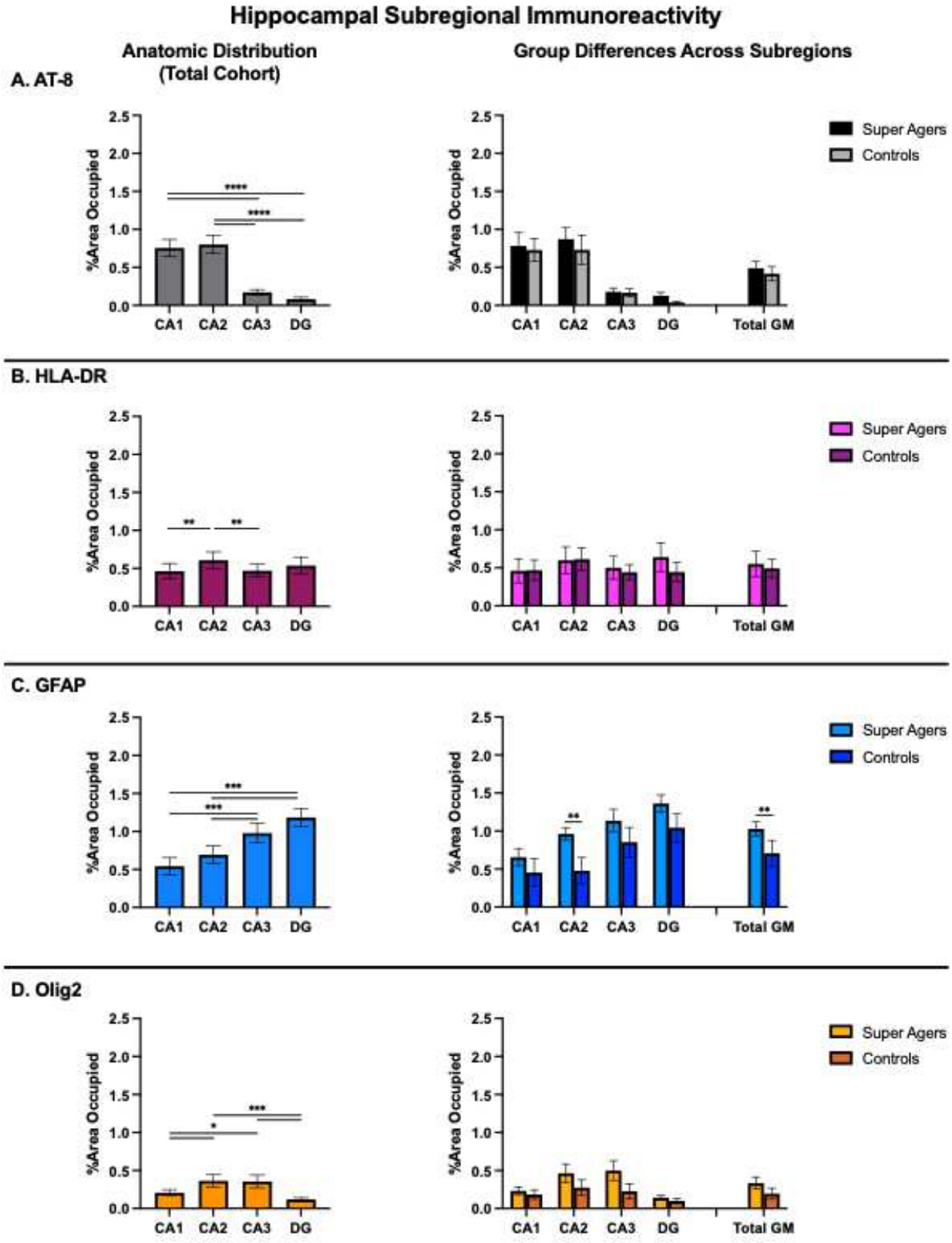


Fig. 3 Hippocampal Subregional Immunoreactivity. A) pTau was significantly higher in the CA1 and CA2 subregion compared to CA3 and DG (both ****$p<0.0001$). **B)** HLA-DR immunoreactivity was

significantly higher in the CA2 than in CA1 and CA3 (**p<0.01). **A-B)** SuperAgers and normal controls did not significantly differ in hippocampal grey matter burden of pTau (%AO by AT-8) or activated microglia (%AO by HLA-DR). **C)** GFAP immunoreactivity was significantly higher in the DG and CA3 compared to the CA1 and CA2 (***p<0.001). Astrocytic reactivity (%AO by GFAP) was significantly greater in SuperAgers than in normal controls across pooled grey matter subregions and in the CA2 (**p<0.01). **D)** Olig2 immunoreactivity was significantly higher in the CA2 and CA3 than in the DG (***p<0.001) and CA1 (*p<0.05). Graphs depict mean and SEM

Hippocampal White Matter Glial Density is Highest in the Fimbria and Alveus in PART.

Qualitatively, outer white matter layers that continue to form the crus of the fornix were most densely occupied by activated microglia (%AO by HLA-DR) (**Fig. 4D, E).** Across all participants (N=19), microglial activation was higher in the fimbria (μ=1.21, SD=0.50) and alveus (μ=1.11, SD=0.46) compared to all other white matter layers: oriens (μ=0.77, SD=0.44), radiatum (μ=0.37, SD=0.20), ml-ott (μ=0.66, SD=0.27), and ml-it (μ=0.49, SD=0.30) (all p<0.001). HLA-DR positivity in the oriens was significantly higher than in the ml-it (p<0.05) and radiatum (p<0.001). HLA-DR + immunoreactivity was significantly higher in the ml-ott than the radiatum (p<0.001). See **Fig. 5A**.

Astrocytic reactivity (%AO of GFAP) was also highest in the fimbria (μ=1.70, SD=0.27) and alveus (μ=1.63, SD=0.24) compared to all other white matter layers (p<0.001). As with microglial activation, astrocytic reactivity was lowest in the radiatum (μ=0.52, SD=0.41), significantly lower than all other white matter layers by ~50%, including the oriens (μ=1.09, SD=0.52), ml-it (μ=0.85, SD=0.56), and ml-ott (μ=1.12, SD=0.48) (all p<0.001). The ml-ott also showed significantly higher astrocytic reactivity than the ml-it layer (p<0.05). See **Fig. 4F, G** and **Fig. 5B**.

There was a layered gradient pattern of increasing oligodendrocyte immunoreactivity from innermost to outermost white matter layers, with outer layers expressing ~2-fold as much %AO by Olig2 (**Fig. 4H, I).** Oligodendrocyte burden was highest in the fimbria (μ=0.94, SD= 0.41), followed by the alveus (μ=0.88, SD=0.32) and oriens (μ=0.75, SD=0.29). The fimbria and alveus showed significantly greater oligodendrocyte immunoreactivity than the ml-it (μ=0.25, SD=0.15), ml-ott (μ=0.61, SD=0.31), and radiatum (μ=0.45, SD=0.27) (all p<0.001). The oriens layer had significantly higher Olig2 + immunoreactivity than the radiatum (p<0.05). The ml-it layer showed significantly lower oligodendrocyte reactivity compared to all other white matter layers (all p<0.05). See **Fig. 4H, I** and **Fig. 5C.**

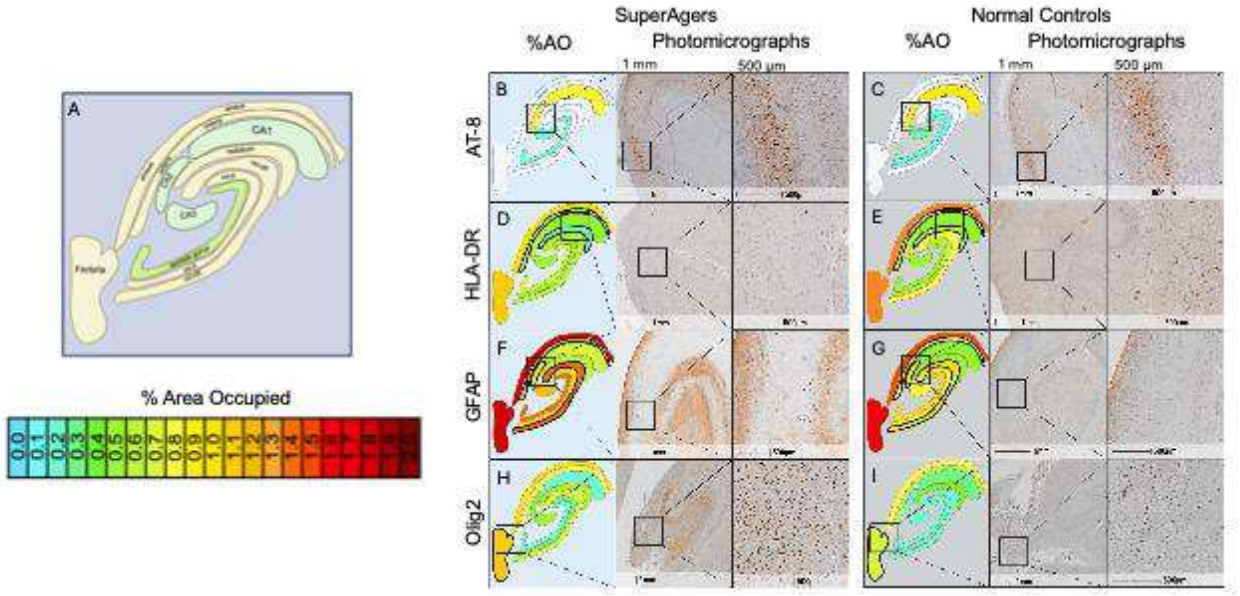


Fig. 4 Heatmap of Tau and Glial Immunoreactivity (%AO) across Hippocampal Regions in Annotation. A) Diagram depicts annotated regions of interest. Grey matter subregions (green) include CA1, CA2, and CA3 pyramidal cells (teal) and dentate gyrus granule cells (light green). White matter layers (yellow) include: fimbria; alveus; oriens; radiatum; ml-ott, stratum lacunosum-moleculare of the dentate gyrus outter two-thirds (ml-ott) and inner third (ml-it). Color gradient depicts low %AO (blue) to high %AO (dark red). Heatmaps depict regional distribution of immunoreactivity in the hippocampus of SuperAgers (left, light blue) and normal controls (right, grey). Regions with significantly different %AO between SuperAgers (left, light blue) and normal controls (right, grey) are outlined in black. Photomicrographs depict pTau (%AO by AT-8) in the CA2 subregion of the hippocampus within a SuperAger **(B)** and normal control **(C)** post-mortem tissue. Within the radiatum and oriens, SuperAgers **(D)** exhibited significantly less activated microglia (%AO by HLA-DR) compared to normal controls **(E)** ($p<0.05$). SuperAgers (**F**) exhibited significantly more astrocytic activation (%AO by GFAP) compared to normal controls **(G)** in the CA2 subregion, and oriens and ml-ott white matter layers ($p<0.05$). Within the fimbria, SuperAgers (**H**) displayed significantly more oligodendroglial cells (%AO by Olig2) than normal controls (**I**) ($p<0.01$). Scale bar = 1 mm (left) and 500 µm (right)

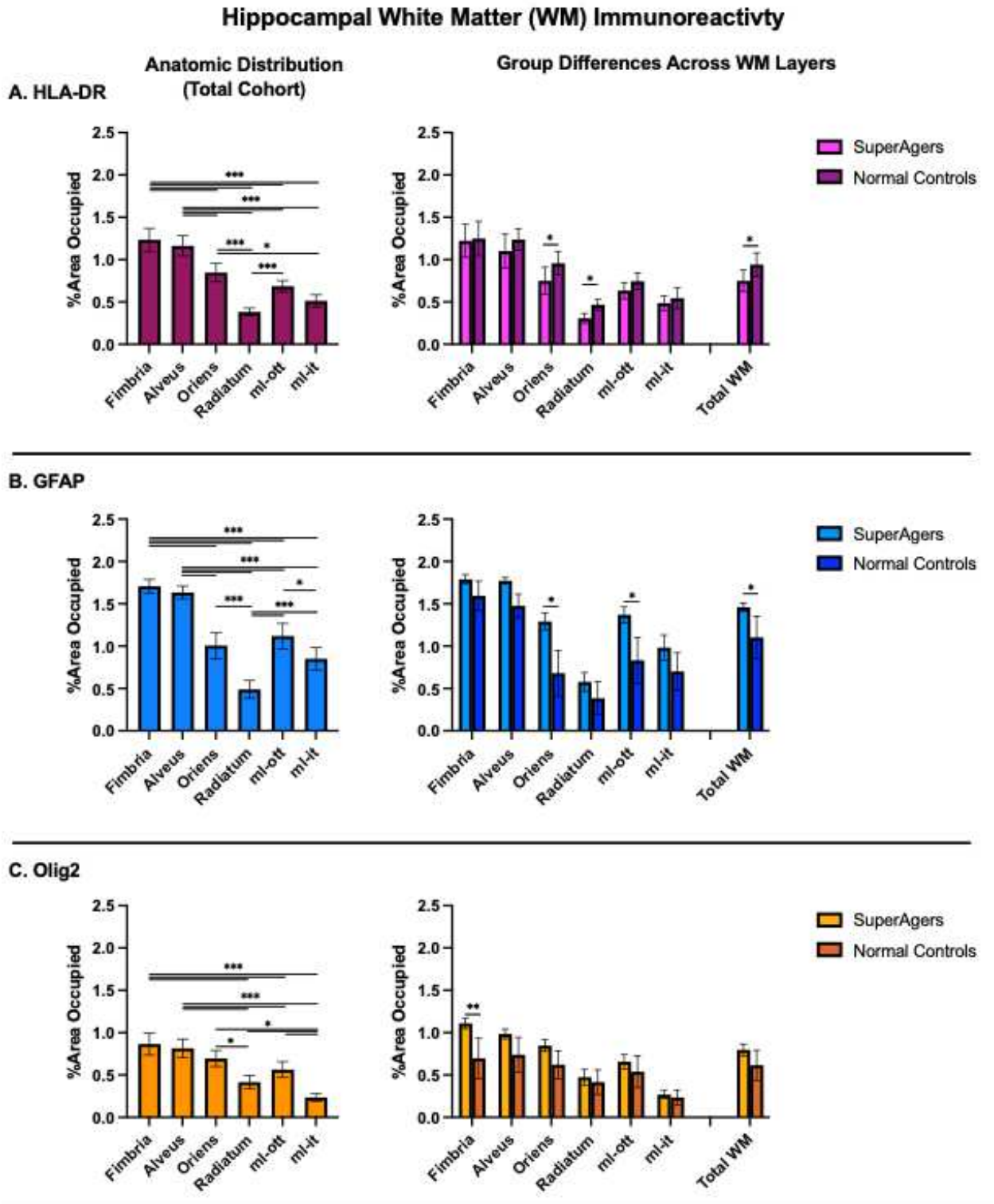


Fig. 5 Hippocampal Immunoreactivity across Defined Subcortical White Matter Layers. A) HLA-DR was higher in the fimbria and alveus compared to oriens, radiatum, ml-ott, and ml-it (*** $p<0.001$). HLA-DR was significantly higher in the oriens compared to the ml-it (*$p<0.05$) and radiatum (***$p<0.001$). HLA-DR + immunoreactivity was higher in the ml-ott than the radiatum (***$p<0.001$).

SuperAgers exhibited significantly less microglial activation (%AO by HLA-DR) compared to normal controls across pooled white matter layers and within the radiatum and oriens (all *p<0.05). **B)** GFAP reactivity was higher in the fimbria and alveus than to oriens, radiatum, ml-ott, and ml-it (all ***p<0.001). Astrocytic immunoreactivity was significantly lower in the radiatum than oriens, ml-it, and ml-ott (all ***p<0.001). The ml-ott showed significantly higher astrocytic reactivity than ml-it layer (*p<0.05). SuperAgers displayed higher astrocytic reactivity (%AO by GFAP) than normal controls across pooled white matter layers and within the oriens and ml-ott (all *p<0.05). **C)** Olig2 immunoreactivity was significantly higher in the fimbria and alveus than ml-it, ml-ott, and radiatum (***p<0.001). Within the ml-it layer, Olig2 immunoreactivity was significantly lower than reactivity in the oriens, radiatum, and ml-ott (all *p<0.05). SuperAgers showed higher oligodendrocyte burden (%AO by Olig2) than normal controls within the fimbria (**p<0.01). Note: ml-it: molecular layer of the dentate gyrus (ml-it); ml-ott: stratum lacunosum-molecular layer; radiatum: stratum radiatum. Graphs depict mean and SEM

Prominent Astrocytic Reactivity in the Hippocampus in PART across all Successful Agers.

Of the %AO by the three glial markers, GFAP demonstrated the highest immunoreactivity in both hippocampal grey matter (μ=1.19, SD=0.51) and white matter (μ=1.38, SD=0.35). In total grey matter, GFAP was significantly greater than HLA-DR %AO (μ=0.51, SD=0.27) and Olig2 (μ=0.64; SD=0.42) (p<0.001) by approximately 2-fold. Across pooled white matter, %AO GFAP was ~1.5x higher than HLA-DR (μ=0.90, SD=0.37) and ~2-fold higher than Olig2 (μ=0.72, SD=0.29) (both p<0.001). SuperAgers and normal controls both showed this pattern of glial activation, i.e., highest GFAP reactivity followed by HLA-DR and Olig2 burden. See **Fig. 6**.

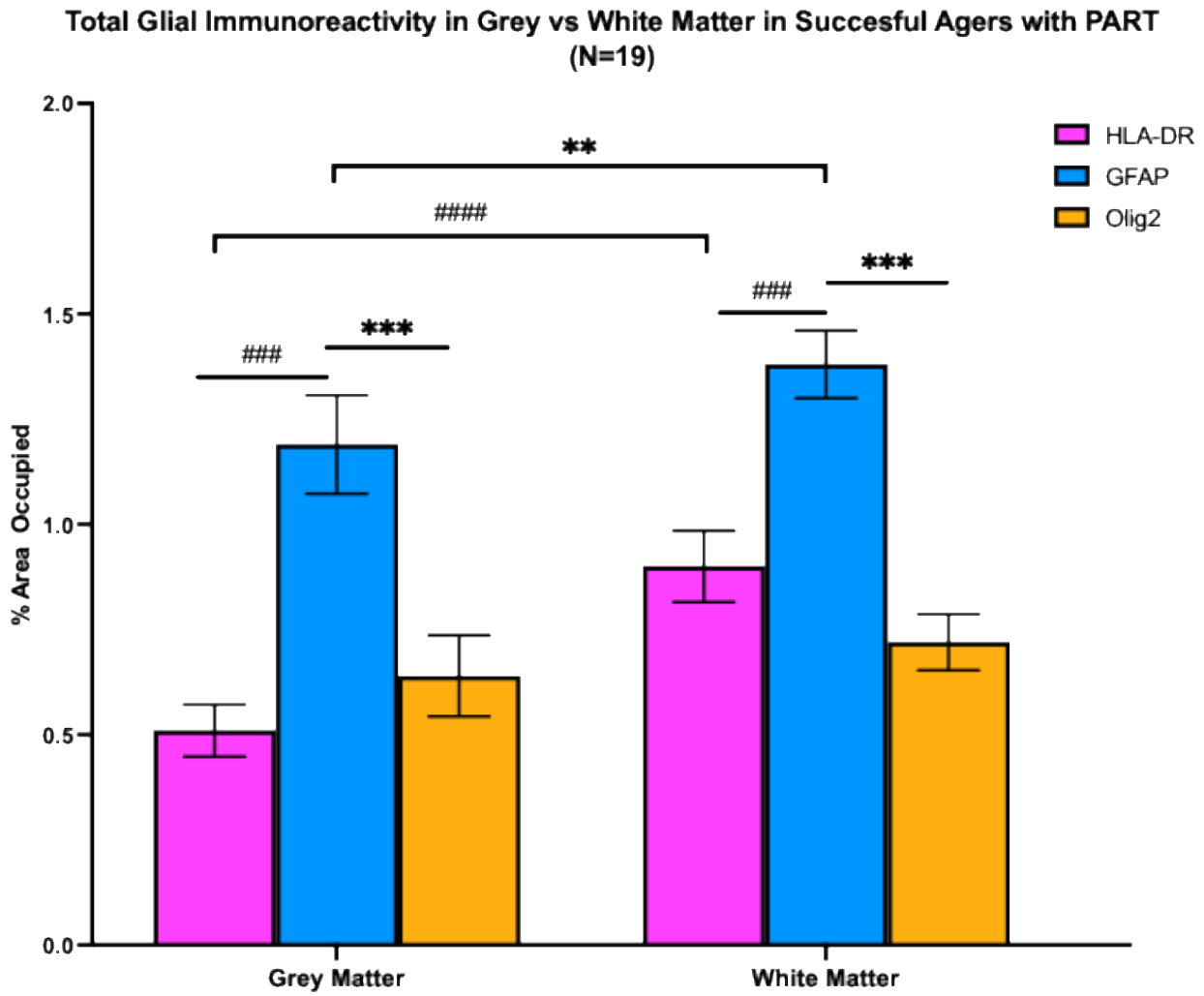


Fig. 6 Total Glial Immunoreactivity in Hippocampal Grey versus White Matter. Microglial (HLA-DR) and astrocytic (GFAP) immunoreactivity were significantly higher in the hippocampal white matter versus grey matter (###p<0.001 and **p<0.01, respectively). Astrocytic immunoreactivity (GFAP) was significantly higher than other glial markers in both the hippocampal grey and white matter, including HLA-DR+ activated microglia ($^{###}p$<0.001) and Olig2+ oligodendrocytes (***p<0.001). Graphs depict mean and SEM

Greater Microglial Activation and Astrocytic Reactivity in Hippocampal White vs. Grey Matter.

Across all participants, HLA-DR immunoreactivity was significantly higher in the total hippocampal white matter (%AO μ=0.90, SD=0.37) compared to the grey matter (μ=0.51, SD=0.27; p<0.001) by approximately 2-fold**.** Astrocytic reactivity (%AO by GFAP) was also higher in the hippocampal white matter (μ=1.38, SD=0.35) than grey matter (μ=1.19, SD=0.51; p<0.01). While significant, the difference was slight by ~15%. Oligodendrocyte burden (%AO by Olig2) was similar between the hippocampal grey matter (μ=0.64, SD=0.42) and white matter (μ=0.72, SD=0.29. See **Fig. 6.** There were no observed

differences between SuperAgers and normal controls in the ratio of grey matter to white matter glial reactivity (HLA-DR, GFAP, or Olig2).

Distinct Hippocampal Glial Patterns in SuperAgers versus Normal Controls with PART.

Level of pTau within discrete hippocampal grey matter subregions did not significantly differ between SuperAgers (total μ=0.53, SD=0.48) and normal controls (total μ=0.54, SD=0.56) (**Fig. 3A & Fig. 4B-C**). In grey matter, there were no observable differences in HLA-DR immunoreactivity (%AO by HLA-DR) between SuperAgers and normal controls (**Fig. 3B & Fig. 4D-E**). In the white matter, however, SuperAgers displayed lower microglial reactivity than normal controls overall (μ=0.64; SD=0.32 vs. μ=0.94; SD=0.36, respectively; $p<0.05$; **Fig. 5A & Fig. 4D-E**). Within the white matter layers of the CA fields, SuperAgers exhibited about half as much microglial activation as normal controls, reaching significance within the radiatum (μ=0.25, SD=0.15 vs. μ=0.52, SD=0.15) and oriens (μ=0.56, SD= 0.36 vs. μ=1.05; SD=0.39) (both $p<0.05$; **Fig. 5A & Fig. 4D-E**). Across total hippocampal grey matter, SuperAgers displayed significantly higher astrocytic reactivity (%AO by GFAP) than normal controls (μ=1.11, SD=0.43 vs. μ=0.79, SD=0.64; $p<0.01$; **Fig. 3C & Fig. 4F-G**). This difference was most evident in the CA2, with approximately 2-fold greater astrocytic reactivity in SuperAgers (μ=0.96, SD=0.23) than in normal controls (μ=0.48, SD=0.54; $p<0.01$). SuperAgers also exhibited greater astrocytic reactivity across the total hippocampal white matter versus normal controls (μ=1.46, SD=0.14 vs μ=1.28, SD=0.52; $p<0.05$; **Fig. 5B & Fig. 4F-G**). This was most notable within the oriens (SuperAgers μ=1.29, SD=0.29 vs. normal controls μ=0.79, SD=0.72; $p<0.05$) and ml-ott (SuperAgers, μ=1.37, SD=0.26 vs. normal controls, μ=0.83, SD=0.72; $p<0.05$). SuperAgers showed an increase in astrocytic reactivity of >60% compared to normal controls within the oriens and ml-ott layers. Groups otherwise did not significantly differ by oligodendrocyte burden in grey matter subregions. In the white matter, outer layers tended to show higher oligodendrocyte immunoreactivity in SuperAgers than in normal controls, significantly more so in the fimbria (μ=1.11, SD=0.06 vs. μ=0.58, SD=0.22 respectively; $p<0.05$; **Fig. 4H-I** & **Fig. 5C**).

Inverse Relationship between pTau Burden and Astrocytic Reactivity in Hippocampal Grey Matter.

We observed a surprising inverse relationship between %AO by pTau and astrocytic reactivity within the hippocampal grey matter subregions (**Fig. 3A, C & Fig. 7A**). Post-hoc analyses with GEE models revealed a significant negative association between %AO of pTau and astrocyte reactivity across the total cohort (N=19, β=-0.35; $p<0.001$), which remained significant when accounting for age at death and Thal phase. Stratified analyses demonstrated similar associations in both SuperAgers ($\beta = -0.42$, $p<0.01$) and normal controls ($\beta = -0.30$, $p<0.05$). Complementary correlation analyses indicated that %AO pTau explained approximately 20% of the variance in hippocampal astrocytic immunoreactivity across the total cohort ($R^2 =0.21$; $p<0.001$) and for both SuperAgers ($R^2 =0.22$; $p<0.01$) and normal controls ($R^2=0.19$; $p<0.05$). No significant associations were observed between pTau and either microglial activation or oligodendrocyte burden. See **Fig. 7.**

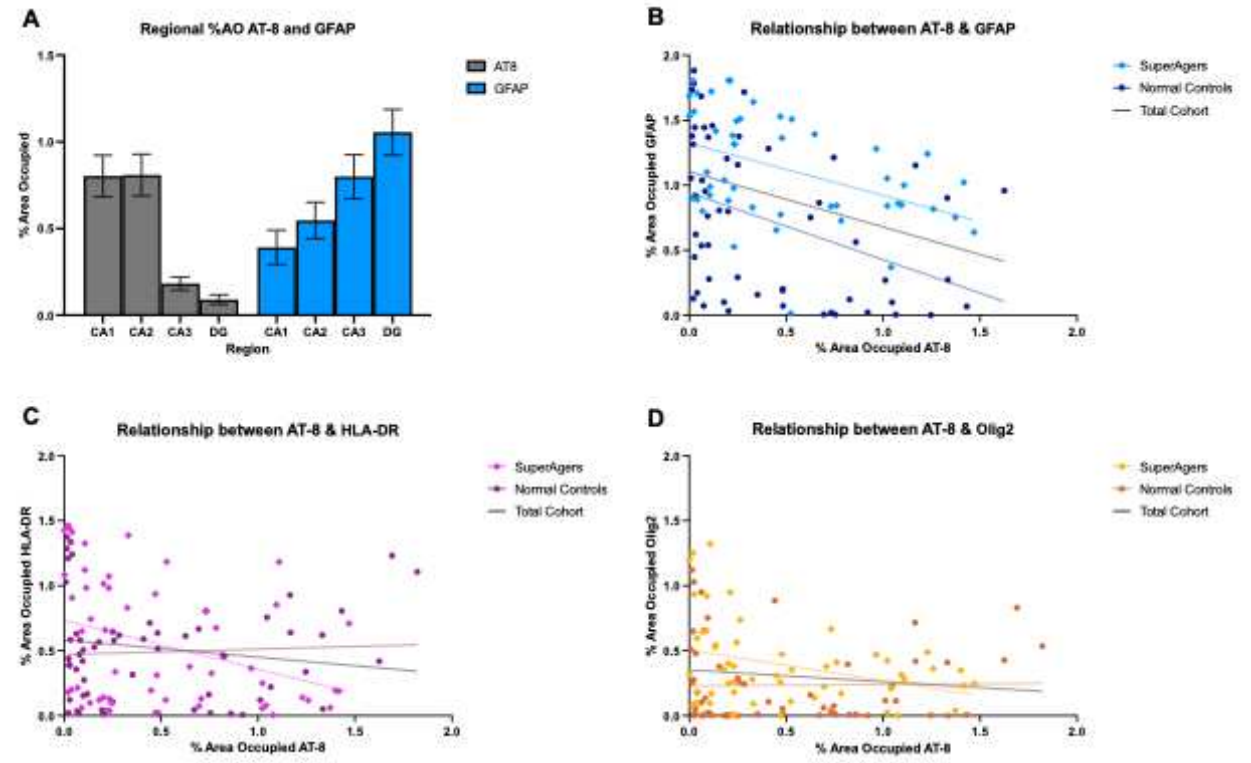


Fig. 7 Relationship between pTau and Glial Immunoreactivity in Grey Matter. A-B) Across grey matter subregions, there was a surprising negative relationship between pTau (%AO by AT-8) and astrocytic immunoreactivity (%AO by GFAP) (β=-0.35, R^2=0.21; p<0.001). Graphs depict mean and SEM. **C)** Microglial activation (%AO by HLA-DR) and **D)** oligodendrocyte burden (%AO by Olig2) were not significantly correlated with level of pTau in hippocampal grey matter

DISCUSSION.

The goal of the current study was to identify distinct region-specific glial signatures in the hippocampus associated with exceptional memory in older adults with primary age-related tauopathy (PART). Across our entire cohort of SuperAgers and their cognitively normal age-matched peers, all with autopsy-confirmed PART, pTau burden was greater in the CA1 and CA2 relative to the CA3 and dentate granule layer. Despite comparable hippocampal pTau burden, SuperAgers, defined by their outstanding memory capacity, differed from their peers across all three glial markers measured: they demonstrated 1) lower HLA-DR+ microglial immunoreactivity in white but not grey matter; 2) greater Olig2+ oligodendrocytic immunoreactivity in the fimbria, and 3) greater GFAP+ astrocytic immunoreactivity in both grey and white matter layers. Across all participants, pTau was inversely associated with GFAP immunoreactivity, whereby lower pTau was linked to higher surrounding astrocytic load. Collectively, these findings suggest that exceptional memory in the presence of PART may depend not only on the severity and distribution of tau pathology, but also on the glial environment that appears to either promote or constrain disease emergence.

It is worth highlighting the overall hippocampal tau and glial landscape observed across the full PART cohort. Within grey matter, the topographic distribution of each marker was distinct: pTau and HLA-DR

were highest in CA1 and CA2, GFAP was highest in the dentate gyrus and CA3, and Olig2 was highest in the CA2 and CA3. Within the white matter, all three glial markers were most densely concentrated to the outer layer regions such as the fimbria and the alveus. GFAP showed the highest immunoreactivity in both hippocampal grey and white matter, exceeding both HLA-DR and Olig2 by approximately 2-fold. HLA-DR and GFAP immunoreactivity were significantly greater in white than grey matter, consistent with prior observations that aging disproportionately affects white matter glia [12, 32, 37, 21]. These subregional and laminar patterns provide a contextual framework for interpreting our SuperAger-specific findings.

Prior studies suggest that SuperAgers may exhibit resistance, defined as absence or attenuation of neuropathology, or resilience, defined as cognitive preservation despite neuropathology [2]. SuperAgers do show neurofibrillary tangles in the entorhinal cortex, albeit at significantly lower levels compared to their cognitively average peers [20], and some harbor substantial neuropathologic burden without the expected cognitive consequences [41, 53]. The current cohort offers an opportunity to examine resilience to hippocampal tau more directly with a focus on contributions of glia. The absence of group differences in hippocampal pTau does not conflict with previous observations of the neuroanatomic specificity of PART. The present study examined discrete hippocampal subfields in individuals with at least normal memory performance, and tau staging restricted to Braak stage IV or lower. The pattern observed—that CA1, and particularly CA2, were areas of highest neurofibrillary tangle presence—is consistent with prior studies that distinguish PART from later stages of pTau accumulation characteristic of the ADNC entity [52, 40].

SuperAgers exhibited approximately twice the Olig2 immunoreactivity of normal controls in the fimbria, together with lower HLA-DR immunoreactivity across hippocampal white matter. In the stratum oriens and radiatum, which contain axonal and dendritic compartments critical to local CA1 and CA2 circuits, SuperAgers showed approximately half as much HLA-DR immunoreactivity as normal controls. We have shown in neocortical, anterior cingulate cortex, and entorhinal cortex that reduced white matter microglia in SuperAgers resembles levels observed in much younger adults [21]. The present findings extend this pattern into the hippocampal formation, despite the presence of PART. Olig2 is expressed throughout the oligodendrocyte lineage and regulates programs involved in oligodendrocyte differentiation, myelin production, and remyelination [57]. Fibers of the alveus converge within the fimbria, the main site of elevated Olig2 expression in Superagers, and are contiguous with the fornix, forming a major conduit for hippocampal afferent and efferent communication. In nondemented older adults, lower fornix myelination has been associated with poorer episodic memory, independent of hippocampal volume and vascular risk [4]. In mice, natural aging has been associated with fewer oligodendrocyte precursor cells and altered OPC–microglial relationships in the fimbria, suggesting this myelin-rich region constitutes an age-sensitive glial niche [22]. Together, our findings suggest a unique white matter glial signature in SuperAgers characterized by greater Olig2, coupled with lower HLA-DR immunoreactivity. This may reflect relative preservation or adaptive remodeling of oligodendroglial support within memory-critical circuitry, potentially in the context of a less activated white-matter immune environment.

Astrocytic (GFAP) reactivity was perhaps the most conspicuous glial feature of SuperAgers in this study, exceeding HLA-DR and Olig2 immunoreactivity as well as GFAP levels in normal controls, despite comparable pTau burden. This regional pattern converges with recent multi-omic findings from the SuperAger hippocampus [16] showing a prominent chromatin-accessibility signature in astrocytes that preserved synaptic adhesion and glutamatergic communication with CA1 neurons and neurogenic cells in SuperAgers and cognitively healthy older adults, distinguishing them from individuals with cognitive impairment and Alzheimer's disease. The concentration of GFAP immunoreactivity within hippocampal laminae that receive and integrate excitatory input may therefore reflect an astrocytic phenotype that supports neurotransmitter homeostasis, synaptic integrity, and plasticity across hippocampal circuits. This is further supported by evidence that astrocytes can link activity in stratum oriens to metaplastic regulation of dentate gyrus molecular-layer synapses [45]. Together, these histologic and multi-omic findings position

a regionally patterned astrocytic signature as an important component of hippocampal resilience in SuperAging.

Across our PART cohort, greater pTau was associated with lower GFAP, an unexpected finding in both SuperAgers and normal controls that remained significant even after accounting for age and Thal phase. In typical amnestic AD, relationships among astrocytic reactivity, tau, and cognition appear to depend partly on Aβ and microglial activation [5, 19]. The glial response to tau likely differs in PART, where substantial Aβ deposition is absent. Alternatively, this inverse relationship may reflect subfield-specific distributions of peak pTau in CA1-2 versus peak GFAP in CA3 and the dentate gyrus, rather than a direct antagonistic relationship between astrocytes and tau. A complementary yet theoretical biological explanation is suggested by the proposed biphasic course of reactive astrogliosis in AD, with an early response preceding substantial pathology, attenuation during prodromal disease, and a second increase during clinical dementia [31]. In cognitively successful individuals with PART, greater GFAP at lower levels of pTau may represent a sustained early astrocytic response that supports tissue homeostasis or constrains tau emergence; as pTau increases, this response may attenuate without the Aβ-associated "second wave" observed in AD [31, 36].

A notable strength of this study is its strict inclusion of longitudinally characterized successful agers over age 80 diagnosed neuropathologically with PART, providing an unusually well-defined clinicopathologic cohort. Another strength of this study is the assessment of three complementary glial markers across multiple hippocampal grey and white matter subregions, offering a regionally resolved glial profile in this memory-relevant region that has not yet been reported in SuperAgers. Several limitations should also be considered. Given the rarity of our cohort features, the sample is small, limiting the ability to examine interactions with factors such as sex, APOE genotype, and cerebrovascular disease. Another limitation is that this study does not compare SuperAgers with PART, with SuperAgers with other or no pathology. Future studies including groups of SuperAgers with other pathologies will be required to determine whether the patterns observed as specific to SuperAgers with PART or a general characteristic of all SuperAgers. The present study also examined glial markers independently and was not designed to interrogate the spatial or functional relationships among astrocytes, microglia, and oligodendroglial-lineage cells. Future multiplexed and spatially resolved studies will be needed to determine how these glial populations interact as an integrated cellular network in the SuperAger hippocampus. Furthermore, each marker carries inherent interpretive constraints. Olig2 does not distinguish mature myelinating oligodendrocytes from precursor populations, and greater Olig2 cannot be equated with greater myelination, warranting further investigation on lineage- and myelin-specific markers. Similarly, GFAP does not identify all astrocytes or define a specific functional state, and increased expression cannot be interpreted as uniformly beneficial or detrimental [17]. Additionally, while microglia are the primary antigen-presenting cells within the brain parenchyma, our panel does not enable us to rule out HLA-DR signal originating from infiltrating immune cells, border-associated macrophages, or rare populations of MHC-II+ astrocytes [44]. Future within-subregion and spatial analyses will also be necessary to clarify whether the inverse pTau-GFAP relationship observed reflects subfield-specific distributions. Finally, the cross-sectional postmortem design precludes determination of whether glial differences precede, accompany, or follow the observed patterns of tau accumulation. Future spatially resolved and cell-state–specific studies will help distinguish regional colocalization from temporal or functional relationships between tau and glia.

In summary, our findings show a cell-type- and region-specific glial pattern in the hippocampus of SuperAgers with PART pathology that includes less HLA-DR immunoreactivity in white matter, greater Olig2 immunoreactivity in the fimbria, and greater GFAP immunoreactivity across both grey and white matter. Astrocytes contribute to oligodendrocyte survival and myelin maintenance, whereas white matter microglia participate in age-related myelin damage, phagocytosis, and lipid handling [32, 37, 50]. The coexistence of greater GFAP and Olig2 coupled with lower HLA-DR raises the possibility that exceptional memory is associated with a glial environment capable of supporting neuronal and axonal function without the degree of white matter immune activation accompanying typical aging. Together, our findings suggest

that exceptional memory in late life may depend not only on resistance to tau accumulation, but on a coordinated glial milieu that preserves vulnerable neurons, axons, and the hippocampal circuits they sustain.

TABLES AND FIGURES

Table 1 Characteristics of SuperAging and Normal Control Participants with PART as Primary Neuropathologic Diagnosis.

Participant	*Age at death (years)*	*Sex*	*PMI (h)*	*Brain weight (g)*	*Braak Stage*	*Thal Phase*	*ApoE*	*Comorbid pathology*
SA1	90	F	4.5	1100	III	0	2,3	Vascular disease with motor microinfarcts
SA2	90	M	9	1120	I	0	3,3	Mild to moderate vascular disease
SA3	84	F	90	1289	II	0	3,3	Remote ischemic infarct, Wallerian degeneration
SA4	90	F	9	1133	III	1	3,3	Mild vascular disease
SA5	90	M	14	1267	II	1	3,4	Moderate vascular disease
SA6	87	M	67	1243	II	2	3,3	
SA7	98	F	4	1175	III	2	3,3	Hypertensive cerebrovascular disease
SA8	85	F	9	1310	III	0	3,3	Moderate vascular disease
SA9	97	F	48.0	1127	III	0	3,3	AGD; Moderate vascular disease
NC 1	90	F	NA	1290	II	0	2,3	Acute infarcts
NC 2	83	F	NA	NA	I	0	NA	
NC 3	95	M	45	1421	III	1	3,3	
NC4	95	M	36	1270	II	1	3,3	Moderate vascular disease
NC 5	93	F	9	1180	III	2	3,3	Vascular disease
NC 6	89	F	9	NA	II	1	NA	
NC 7	98	M	12	NA	II	1	NA	
NC 8	87	F	10	1300	III	1	NA	History of seizures
NC 9	107	F	8	NA	II	1	NA	
NC 10	92	F	12	1314	IV	0	2,4	

SA, SuperAger; NC, normal control; PART, primary age-related tauopathy; PMI, post-mostem interval; AGD, argyrophilic grain disease; NA, not available; F, female; M, male; h, hours; g, grams; ApoE, Apolipoprotein E. Braak staging followed published guidelines [7, 8, 10]. Thal phase followed published guidelines [49]

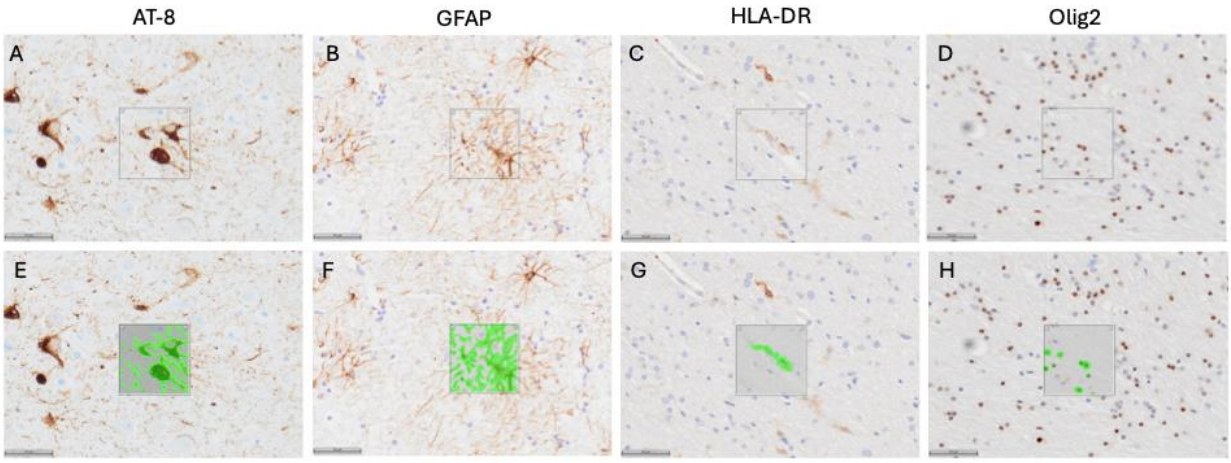


Fig. 1 Immunostaining for phosphorylated tau and glial response in the hippocampus in PART. Photomicrographs of hippocampal staining for AT-8 **(A, E),** GFAP **(B, F),** HLA-DR **(C, G)**, and Olig2 **(D, H)** are depicted in the top row. The bottom row depicts corresponding overlays of the HALO MiniNet Classifier AI algorithm. Scale bar = 50 µm

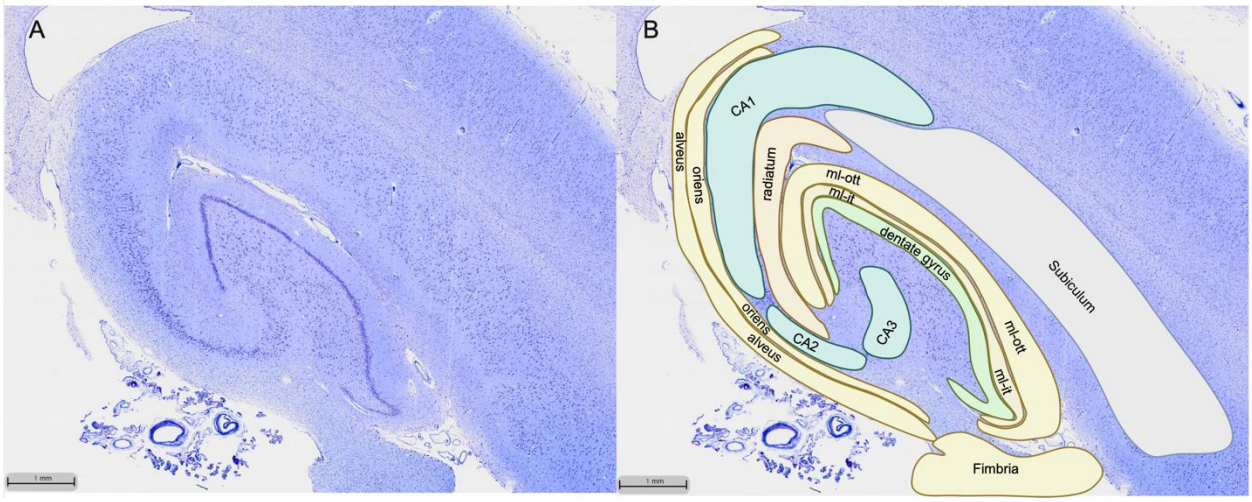


Fig. 2 Hippocampal Subregions of Interest. A) Photomicrograph of a SuperAger's hippocampus stained with CV to visualize neurons. **B)** Annotations of the hippocampal subregions of interest are demonstrated [43, 55]. Grey matter subregions (green) include the CA1, CA2, and CA3, consisting of pyramidal cells (teal), and the granule cells of the dentate gyrus (light green). White matter layers are depicted in yellow. Directly above the granule layer is the inner third of the molecular layer of the dentate gyrus (ml-it), surrounded by the stratum lacunosum-moleculare layer (ml-ott). The stratum radiatum (radiatum) abuts the CA1 and CA2 subregions. The axonal projections of the pyramidal cells are primarily found in the stratum oriens (oriens) and the medial adjacent alveus, which then bundle to form the fimbria. The fimbria is the medial hippocampus white matter bundle that travels posterior-superiorly to form the crus of the fornix. Scale bar = 1 mm

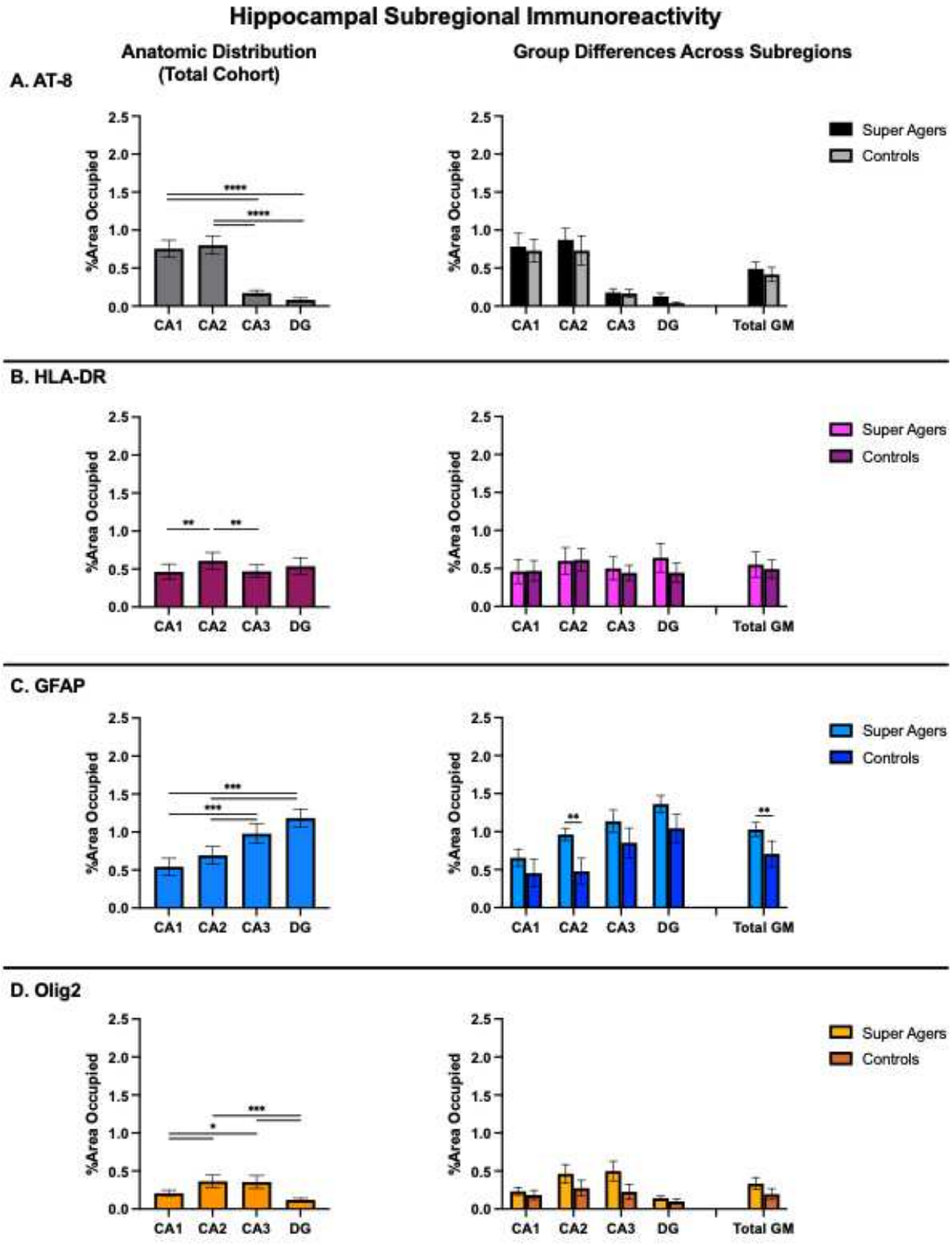

Hippocampal Subregional Immunoreactivity
Anatomic Distribution (Total Cohort)
Group Differences Across Subregions
A. AT-8
B. HLA-DR
C. GFAP
D. Olig2
%Area Occupied
CA1
CA2
CA3
DG
Total GM
Super Agers
Controls

Fig. 3 Hippocampal Subregional Immunoreactivity. A) pTau was significantly higher in the CA1 and CA2 subregion compared to CA3 and DG (both ****$p<0.0001$). **B)** HLA-DR immunoreactivity was significantly higher in the CA2 than in CA1 and CA3 (**$p<0.01$). **A-B)** SuperAgers and normal controls did not significantly differ in hippocampal grey matter burden of pTau (%AO by AT-8) or activated microglia (%AO by HLA-DR). **C)** GFAP immunoreactivity was significantly higher in the DG and CA3 compared to the CA1 and CA2 (***$p<0.001$). Astrocytic reactivity (%AO by GFAP) was significantly greater in SuperAgers than in normal controls across pooled grey matter subregions and in the CA2 (**$p<0.01$). **D)** Olig2 immunoreactivity was significantly higher in the CA2 and CA3 than in the DG (***$p<0.001$) and CA1 (*$p<0.05$). Graphs depict mean and SEM

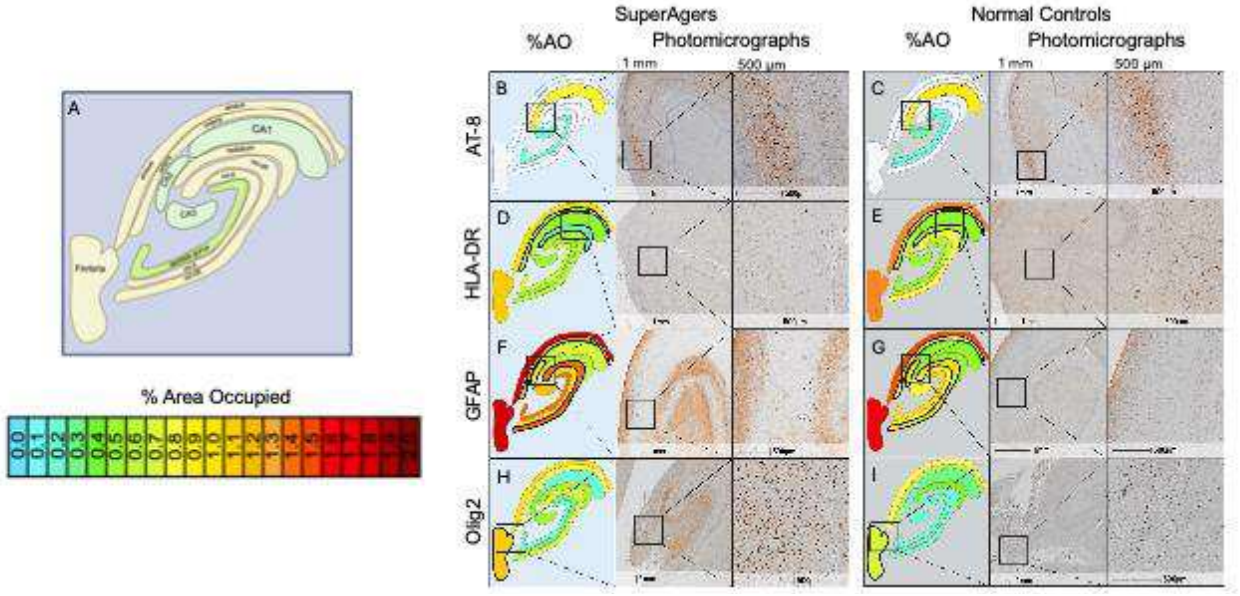


Fig. 4 Heatmap of Tau and Glial Immunoreactivity (%AO) across Hippocampal Regions in Annotation. A) Diagram depicts annotated regions of interest. Grey matter subregions (green) include CA1, CA2, and CA3 pyramidal cells (teal) and dentate gyrus granule cells (light green). White matter layers (yellow) include: fimbria; alveus; oriens; radiatum; ml-ott, stratum lacunosum-moleculare of the dentate gyrus outter two-thirds (ml-ott) and inner third (ml-it). Color gradient depicts low %AO (blue) to high %AO (dark red). Heatmaps depict regional distribution of immunoreactivity in the hippocampus of SuperAgers (left, light blue) and normal controls (right, grey). Regions with significantly different %AO between SuperAgers (left, light blue) and normal controls (right, grey) are outlined in black. Photomicrographs depict pTau (%AO by AT-8) in the CA2 subregion of the hippocampus within a SuperAger **(B)** and normal control **(C)** post-mortem tissue. Within the radiatum and oriens, SuperAgers **(D)** exhibited significantly less activated microglia (%AO by HLA-DR) compared to normal controls **(E)** ($p<0.05$). SuperAgers (**F**) exhibited significantly more astrocytic activation (%AO by GFAP) compared to normal controls **(G)** in the CA2 subregion, and oriens and ml-ott white matter layers ($p<0.05$). Within the fimbria, SuperAgers (**H**) displayed significantly more oligodendroglial cells (%AO by Olig2) than normal controls (**I**) ($p<0.01$). Scale bar = 1 mm (left) and 500 µm (right)

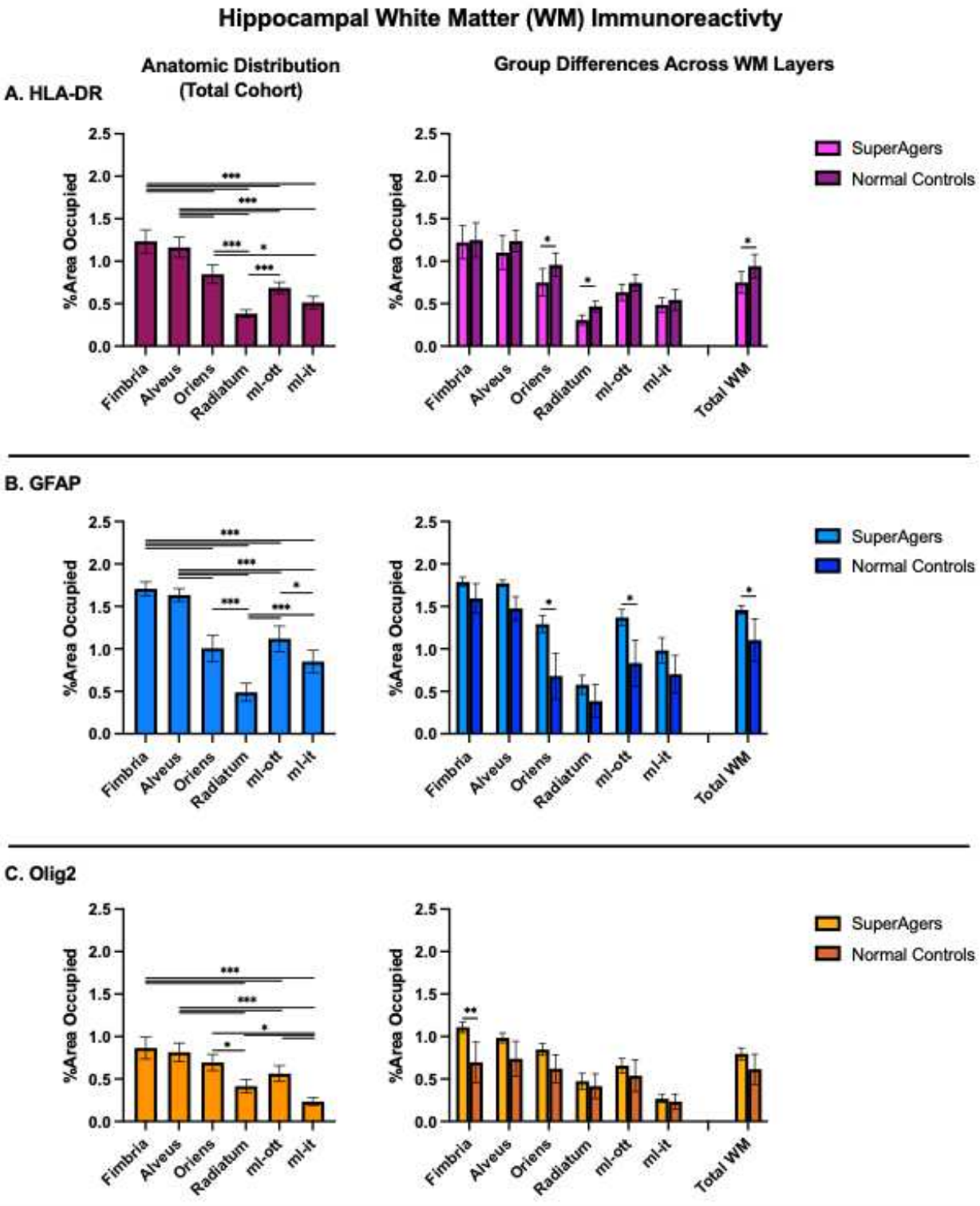

Hippocampal White Matter (WM) Immunoreactivty
Anatomic Distribution (Total Cohort)
Group Differences Across WM Layers
A. HLA-DR
B. GFAP
C. Olig2
%Area Occupied
Fimbria
Alveus
Oriens
Radiatum
ml-ott
ml-it
Total WM
SuperAgers
Normal Controls

Fig. 5 Hippocampal Immunoreactivity across Defined Subcortical White Matter Layers. A) HLA-DR was higher in the fimbria and alveus compared to oriens, radiatum, ml-ott, and ml-it (*** $p<0.001$). HLA-DR was significantly higher in the oriens compared to the ml-it (*$p<0.05$) and radiatum (***$p<0.001$). HLA-DR + immunoreactivity was higher in the ml-ott than the radiatum (***$p<0.001$). SuperAgers exhibited significantly less microglial activation (%AO by HLA-DR) compared to normal controls across pooled white matter layers and within the radiatum and oriens (all *$p<0.05$). **B)** GFAP reactivity was higher in the fimbria and alveus than to oriens, radiatum, ml-ott, and ml-it (all ***$p<0.001$). Astrocytic immunoreactivity was significantly lower in the radiatum than oriens, ml-it, and ml-ott (all ***$p<0.001$). The ml-ott showed significantly higher astrocytic reactivity than ml-it layer (*$p<0.05$). SuperAgers displayed higher astrocytic reactivity (%AO by GFAP) than normal controls across pooled white matter layers and within the oriens and ml-ott (all *$p<0.05$). **C)** Olig2 immunoreactivity was significantly higher in the fimbria and alveus than ml-it, ml-ott, and radiatum (***$p<0.001$). Within the ml-it layer, Olig2 immunoreactivity was significantly lower than reactivity in the oriens, radiatum, and ml-ott (all *$p<0.05$). SuperAgers showed higher oligodendrocyte burden (%AO by Olig2) than normal controls within the fimbria (**$p<0.01$). Note: ml-it: molecular layer of the dentate gyrus (ml-it); ml-ott: stratum lacunosum-molecular layer; radiatum: stratum radiatum. Graphs depict mean and SEM

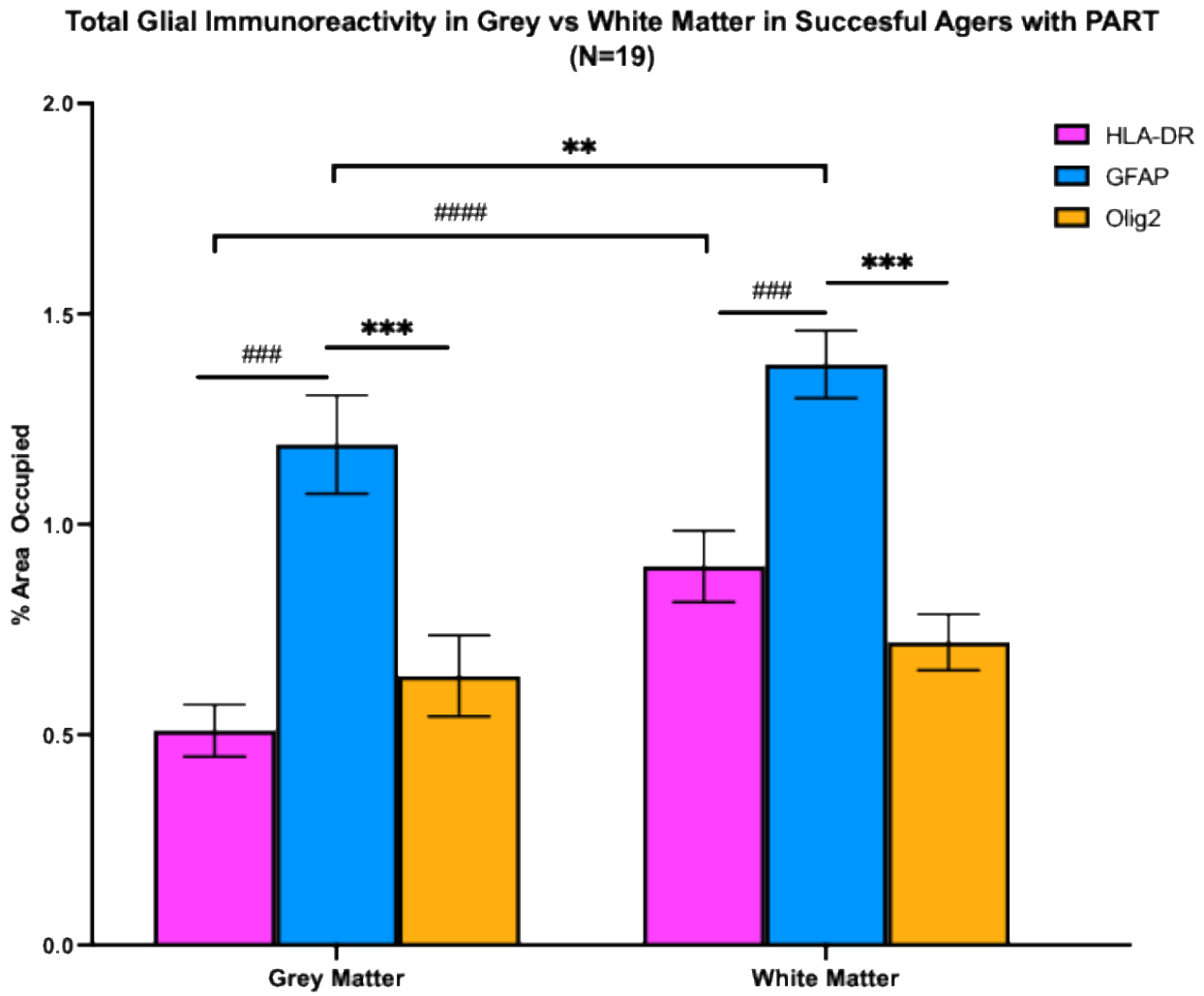


Fig. 6 Total Glial Immunoreactivity in Hippocampal Grey versus White Matter. Microglial (HLA-DR) and astrocytic (GFAP) immunoreactivity were significantly higher in the hippocampal white matter versus grey matter (###p<0.001 and **p<0.01, respectively). Astrocytic immunoreactivity (GFAP) was significantly higher than other glial markers in both the hippocampal grey and white matter, including HLA-DR+ activated microglia ($^{###}p$<0.001) and Olig2+ oligodendrocytes (***p<0.001). Graphs depict mean and SEM

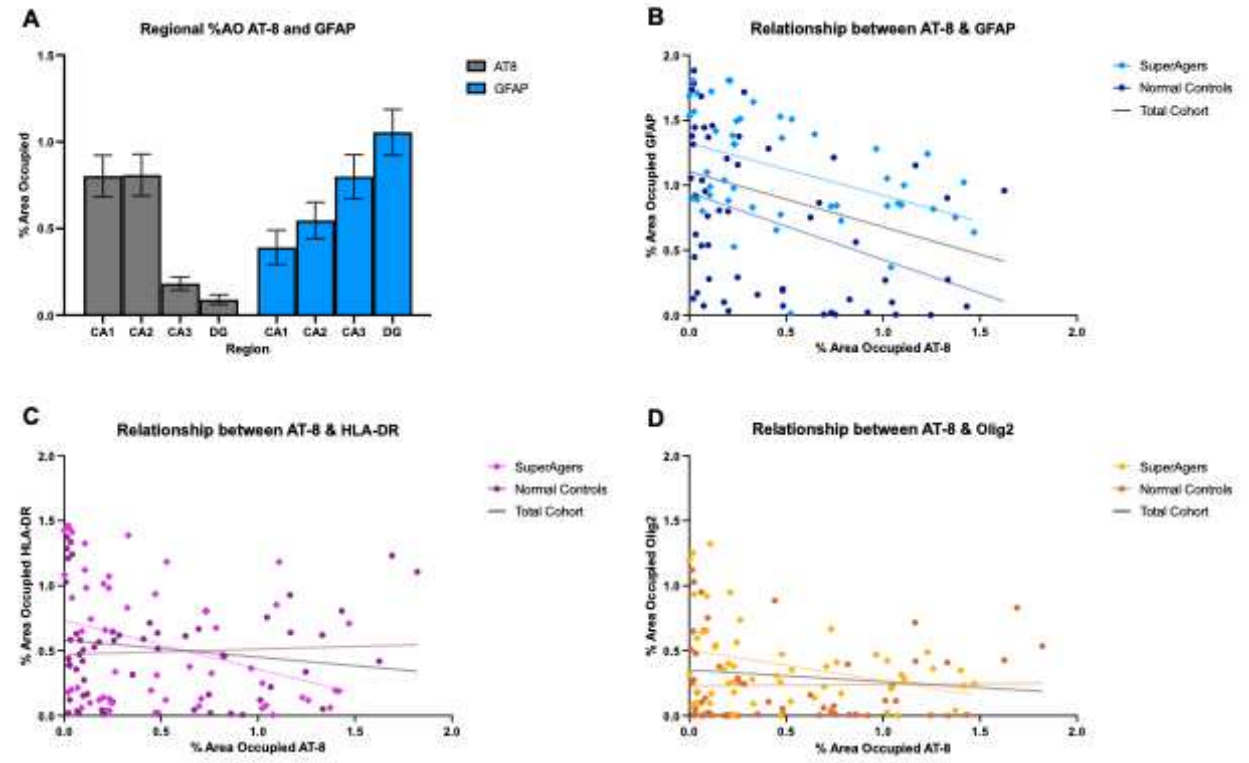


Fig. 7 Relationship between pTau and Glial Immunoreactivity in Grey Matter. A-B) Across grey matter subregions, there was a surprising negative relationship between pTau (%AO by AT-8) and astrocytic immunoreactivity (%AO by GFAP) (β=-0.35, R^2=0.21; p<0.001). Graphs depict mean and SEM. **C)** Microglial activation (%AO by HLA-DR) and **D)** oligodendrocyte burden (%AO by Olig2) were not significantly correlated with level of pTau in hippocampal grey matter

REFERENCES

1. Albert, M. S., et al. (2011). "The diagnosis of mild cognitive impairment due to Alzheimer's disease: recommendations from the National Institute on Aging-Alzheimer's Association workgroups on diagnostic guidelines for Alzheimer's disease." Alzheimers Dement **7**(3): 270-279.
2. Arenaza-Urquijo, E. M. and P. Vemuri (2018). "Resistance vs resilience to Alzheimer disease: Clarifying terminology for preclinical studies." Neurology **90**(15): 695-703.
3. Bancher, C. and K. A. Jellinger (1994). "Neurofibrillary tangle predominant form of senile dementia of Alzheimer type: a rare subtype in very old subjects." Acta Neuropathol **88**(6): 565-570.
4. Bangen, K. J., et al. (2021). "Decreased myelin content of the fornix predicts poorer memory performance beyond vascular risk, hippocampal volume, and fractional anisotropy in nondemented older adults." Brain Imaging Behav **15**(5): 2563-2571.
5. Bellaver, B., et al. (2023). "Astrocyte reactivity influences amyloid-beta effects on tau pathology in preclinical Alzheimer's disease." Nat Med **29**(7): 1775-1781.
6. Braak, H., et al. (2006). "Staging of Alzheimer disease-associated neurofibrillary pathology using paraffin sections and immunocytochemistry." Acta Neuropathol **112**(4): 389-404.

7. Braak, H. and E. Braak (1985). "On areas of transition between entorhinal allocortex and temporal isocortex in the human brain. Normal morphology and lamina-specific pathology in Alzheimer's disease." Acta Neuropathol **68**(4): 325-332.
8. Braak, H. and E. Braak (1991). "Neuropathological stageing of Alzheimer-related changes." Acta Neuropathol **82**(4): 239-259.
9. Braak, H. and E. Braak (1992). "The human entorhinal cortex: normal morphology and lamina-specific pathology in various diseases." Neurosci Res **15**(1-2): 6-31.
10. Braak, H., et al. (1993). "Staging of Alzheimer-related cortical destruction." Eur Neurol **33**(6): 403-408.
11. Bu, G. (2009). "Apolipoprotein E and its receptors in Alzheimer's disease: pathways, pathogenesis and therapy." Nat Rev Neurosci **10**(5): 333-344.
12. Conde, J. R. and W. J. Streit (2006). "Microglia in the aging brain." J Neuropathol Exp Neurol **65**(3): 199-203.
13. Conejero-Goldberg, C., et al. (2014). "APOE2 enhances neuroprotection against Alzheimer's disease through multiple molecular mechanisms." Mol Psychiatry **19**(11): 1243-1250.
14. Corder, E. H., et al. (1993). "Gene dose of apolipoprotein E type 4 allele and the risk of Alzheimer's disease in late onset families." Science **261**(5123): 921-923.
15. Crary, J. F., et al. (2014). "Primary age-related tauopathy (PART): a common pathology associated with human aging." Acta Neuropathol **128**(6): 755-766.
16. Disouky, A., et al. (2026). "Human hippocampal neurogenesis in adulthood, ageing and Alzheimer's disease." Nature.
17. Escartin, C., et al. (2021). "Reactive astrocyte nomenclature, definitions, and future directions." Nat Neurosci **24**(3): 312-325.
18. Farrer, L. A., et al. (1997). "Effects of age, sex, and ethnicity on the association between apolipoprotein E genotype and Alzheimer disease. A meta-analysis. APOE and Alzheimer Disease Meta Analysis Consortium." JAMA **278**(16): 1349-1356.
19. Ferrari-Souza, J. P., et al. (2026). "Microglia modulate Abeta-dependent astrocyte reactivity in Alzheimer's disease." Nat Neurosci **29**(1): 81-87.
20. Gefen, T., et al. (2021). "Paucity of Entorhinal Cortex Pathology of the Alzheimer's Type in SuperAgers with Superior Memory Performance." Cereb Cortex **31**(7): 3177-3183.
21. Gefen, T., et al. (2019). "Activated Microglia in Cortical White Matter Across Cognitive Aging Trajectories." Front Aging Neurosci **11**: 94.
22. Gomez, P. T., et al. (2024). "Aging and senescent fates of oligodendrocyte precursor cells in the mouse brain." NPJ Aging **10**(1): 47.
23. Harrison, T. M., et al. (2012). "Superior memory and higher cortical volumes in unusually successful cognitive aging." J Int Neuropsychol Soc **18**(6): 1081-1085.
24. Heaton, R. K., et al. (2004). Revised comprehensive norms for an expanded Halstead-Reitan battery : demographically adjusted neuropsychological norms for African American and Caucasian adults, professional manual. Lutz, Fla., Psychological Assessment Resources.
25. Hickman, R. A., et al. (2020). "Primary Age-Related Tauopathy (PART): Addressing the Spectrum of Neuronal Tauopathic Changes in the Aging Brain." Curr Neurol Neurosci Rep **20**(9): 39.
26. Hiya, S., et al. (2025). "Unraveling the clinical-pathological correlations of subjects with isolated and mixed neurodegenerative processes in the National Alzheimer's Coordinating Center dataset." J Neuropathol Exp Neurol **84**(3): 177-194.
27. Ikeda, K., et al. (1999). "Clinical aspects of 'senile dementia of the tangle type'-- a subset of dementia in the senium separable from late-onset Alzheimer's disease." Dement Geriatr Cogn Disord **10**(1): 6-11.
28. Itoh, et al. (1996). "Dementia characterized by abundant neurofibrillary tangles and scarce senile plaques: a quantitative pathological study." Eur Neurol **36**(2): 94-97.
29. Ivnik, R. J., et al. (1996). "Neuropsychological tests' norms above age 55: COWAT, BNT, MAE token, WRAT-R reading, AMNART, STROOP, TMT, and JLO." Clinical Neuropsychologist **10**(3): 262-278.

30. Kovacs, G. G., et al. (2016). "Aging-related tau astrogliopathy (ARTAG): harmonized evaluation strategy." Acta Neuropathol **131**(1): 87-102.
31. Kumar, A., et al. (2023). "Reactive astrogliosis: A friend or foe in the pathogenesis of Alzheimer's disease." J Neurochem **164**(3): 309-324.
32. Lundgaard, I., et al. (2014). "White matter astrocytes in health and disease." Neuroscience **276**: 161-173.
33. Minogue, G., et al. (2023). "Distinct Patterns of Hippocampal Pathology in Alzheimer's Disease with Transactive Response DNA-binding Protein 43." Ann Neurol **94**(6): 1036-1047.
34. Morris, J. C., et al. (1989). "The Consortium to Establish a Registry for Alzheimer's Disease (CERAD). Part I. Clinical and neuropsychological assessment of Alzheimer's disease." Neurology **39**(9): 1159-1165.
35. Nassif, C., et al. (2022). "Integrity of Neuronal Size in the Entorhinal Cortex Is a Biological Substrate of Exceptional Cognitive Aging." J Neurosci **42**(45): 8587-8594.
36. Phillips, J. M., et al. (2024). "Pathologic and clinical correlates of region-specific brain GFAP in Alzheimer's disease." Acta Neuropathol **148**(1): 69.
37. Raj, D., et al. (2017). "Increased White Matter Inflammation in Aging- and Alzheimer's Disease Brain." Front Mol Neurosci **10**: 206.
38. Reiman, E. M., et al. (2020). "Exceptionally low likelihood of Alzheimer's dementia in APOE2 homozygotes from a 5,000-person neuropathological study." Nat Commun **11**(1): 667.
39. Reitan, R. M. (1958). "Validity of the Trail Making Test as an Indicator of Organic Brain Damage." Perceptual and Motor Skills **8**(3): 271-276.
40. Richardson, T. E., et al. (2025). "Primary age-related tauopathy." Acta Neuropathol **150**(1): 40.
41. Rogalski, E., et al. (2019). "Cognitive trajectories and spectrum of neuropathology in SuperAgers: The first 10 cases." Hippocampus **29**(5): 458-467.
42. Rogalski, E. J., et al. (2013). "Youthful memory capacity in old brains: anatomic and genetic clues from the Northwestern SuperAging Project." J Cogn Neurosci **25**(1): 29-36.
43. Rosene, D. L. and G. W. Van Hoesen (1987). The Hippocampal Formation of the Primate Brain. Cerebral Cortex: Further Aspects of Cortical Function, Including Hippocampus. E. G. Jones and A. Peters. Boston, MA, Springer US**:** 345-456.
44. Rostami, J., et al. (2020). "Astrocytes have the capacity to act as antigen-presenting cells in the Parkinson's disease brain." J Neuroinflammation **17**(1): 119.
45. Sateesh, S., et al. (2026). "Transregional astrocyte-dependent metaplasticity in the hippocampus." Proc Natl Acad Sci U S A **123**(28): e2536065123.
46. Saxton, J., et al. (2000). "Normative data on the Boston Naming Test and two equivalent 30-item short forms." Clinical Neuropsychologist **14**(4): 526-534.
47. Schmidt, M. (1996). Rey Auditory Verbal Learning Test: RAVLT : a Handbook, Western Psychological Services.
48. Shirk, S. D., et al. (2011). "A web-based normative calculator for the uniform data set (UDS) neuropsychological test battery." Alzheimers Res Ther **3**(6): 32.
49. Thal, D. R., et al. (2002). "Phases of A beta-deposition in the human brain and its relevance for the development of AD." Neurology **58**(12): 1791-1800.
50. Tognatta, R., et al. (2020). "Astrocytes Are Required for Oligodendrocyte Survival and Maintenance of Myelin Compaction and Integrity." Front Cell Neurosci **14**: 74.
51. Ulrich, J. (1992). "Abundant neurofibrillary tangles without senile plaques in a subset of patients with senile dementia." Neurodegeneration **1**: 257-264.
52. Walker, J. M., et al. (2021). "Early Selective Vulnerability of the CA2 Hippocampal Subfield in Primary Age-Related Tauopathy." J Neuropathol Exp Neurol **80**(2): 102-111.
53. Weintraub, S., et al. (2025). "The first 25 years of the Northwestern University SuperAging Program." Alzheimers Dement **21**(8): e70312.
54. Weintraub, S., et al. (2009). "The Alzheimer's Disease Centers' Uniform Data Set (UDS): the neuropsychologic test battery." Alzheimer Dis Assoc Disord **23**(2): 91-101.

55. Williams, E. M., et al. (2023). "Pentad: A reproducible cytoarchitectonic protocol and its application to parcellation of the human hippocampus." Frontiers in Neuroanatomy **17**.
56. Yokota, O., et al. (2018). "Neuropathological comorbidity associated with argyrophilic grain disease." Neuropathology **38**(1): 82-97.
57. Zhang, K., et al. (2022). "Author Correction: The Oligodendrocyte Transcription Factor 2 OLIG2 regulates transcriptional repression during myelinogenesis in rodents." Nat Commun **13**(1): 3164.